SUPPORTING INFORMATION

Exploring the interaction between a fluorescent Ag(I)-biscarbene complex and non-canonical DNA structures: a multi-technique investigation

Francesca Binacchi, Ester Giorgi, Giacomo Salvadori, Damiano Cirri, Mariassunta Stifano, Aurora Donati, Linda Garzella, Natalia Busto, Begona Garcia, Alessandro Pratesi, Tarita Biver

Table of Contents

NMR spectra

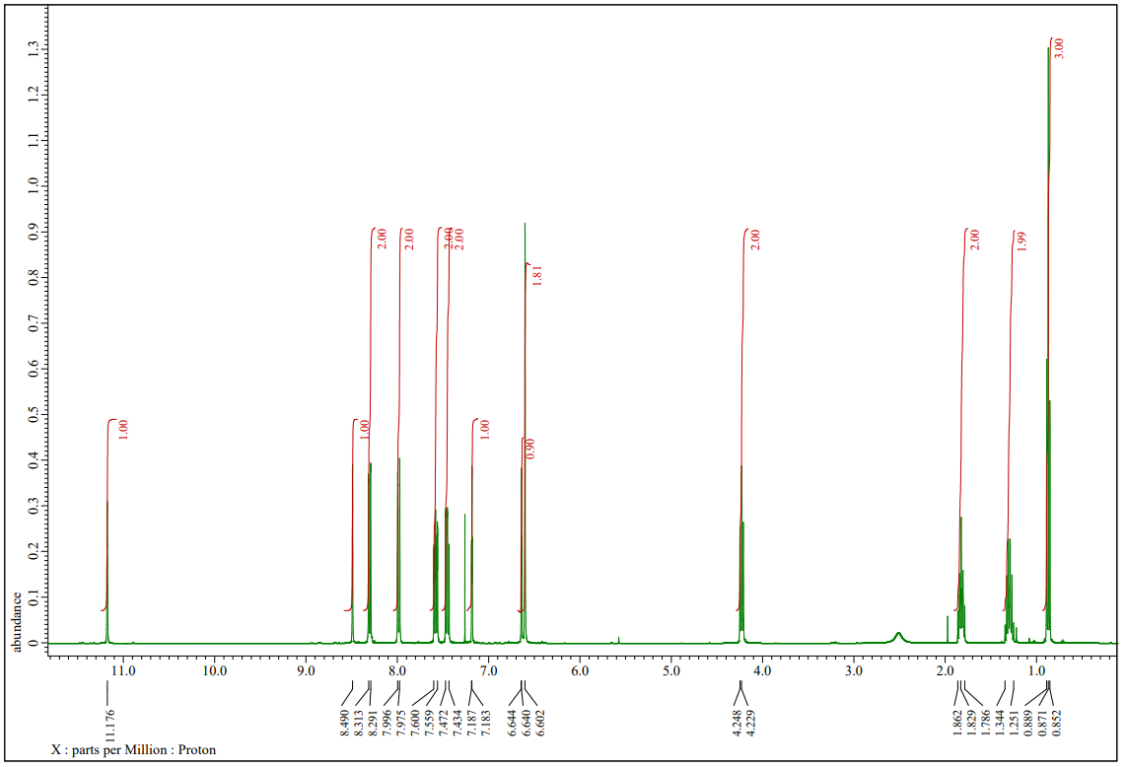

Figure S1 1-(anthracen-9-ylmethyl)-3-butylimidazolium chloride, BIA **(1)**, ^{1}H NMR

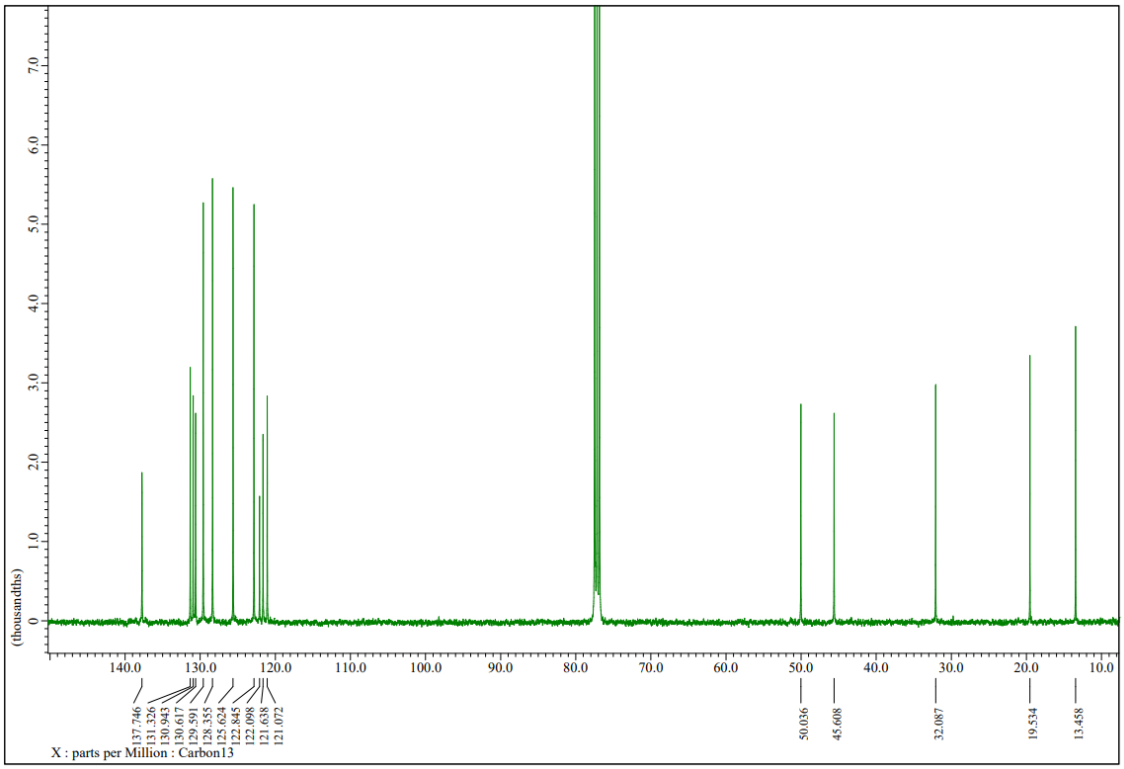

Figure S2 1-(anthracen-9-ylmethyl)-3-butylimidazolium chloride, BIA **(1)**, ^{13}C NMR

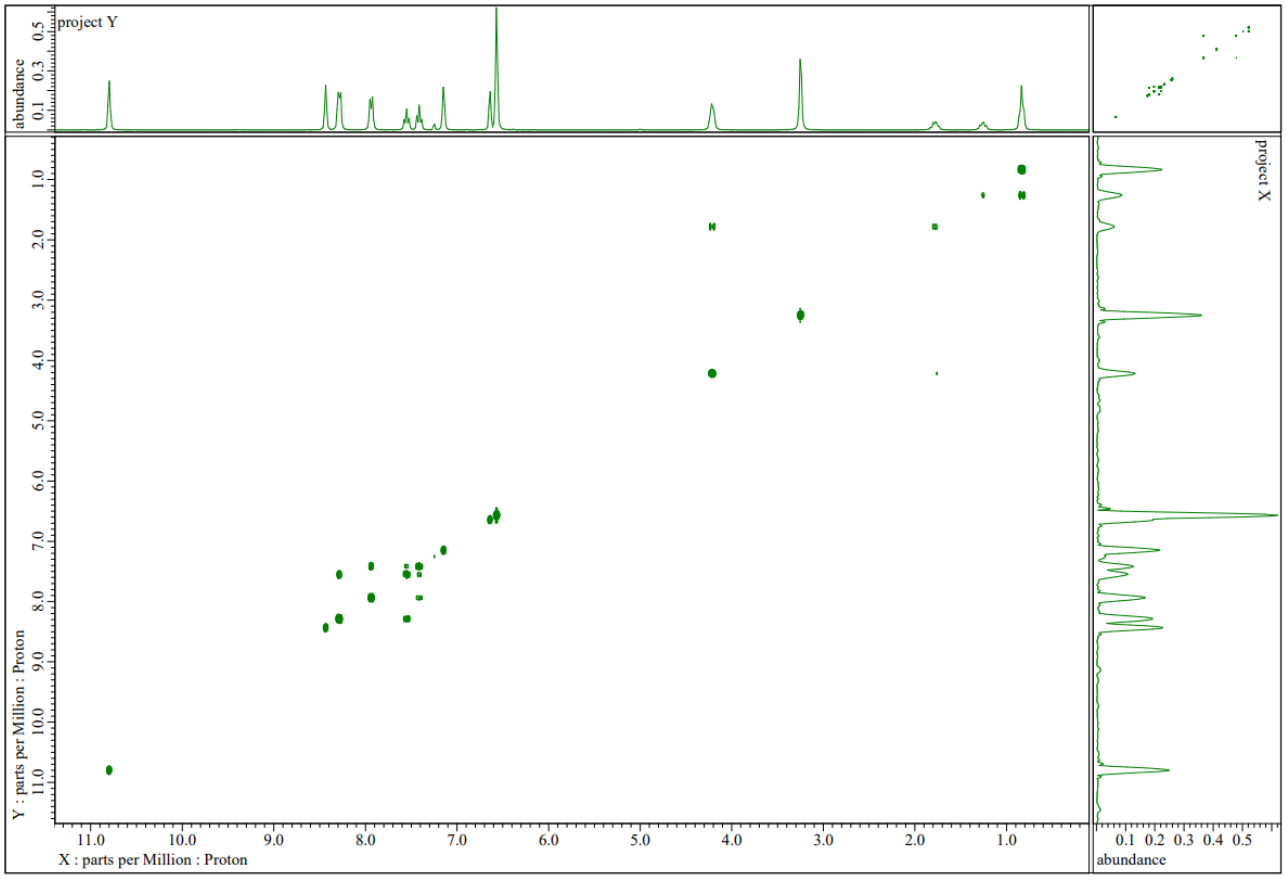

Figure S3 1-(anthracen-9-ylmethyl)-3-butylimidazolium chloride, BIA **(1)**, ^{1}H-^{1}H COSY NMR

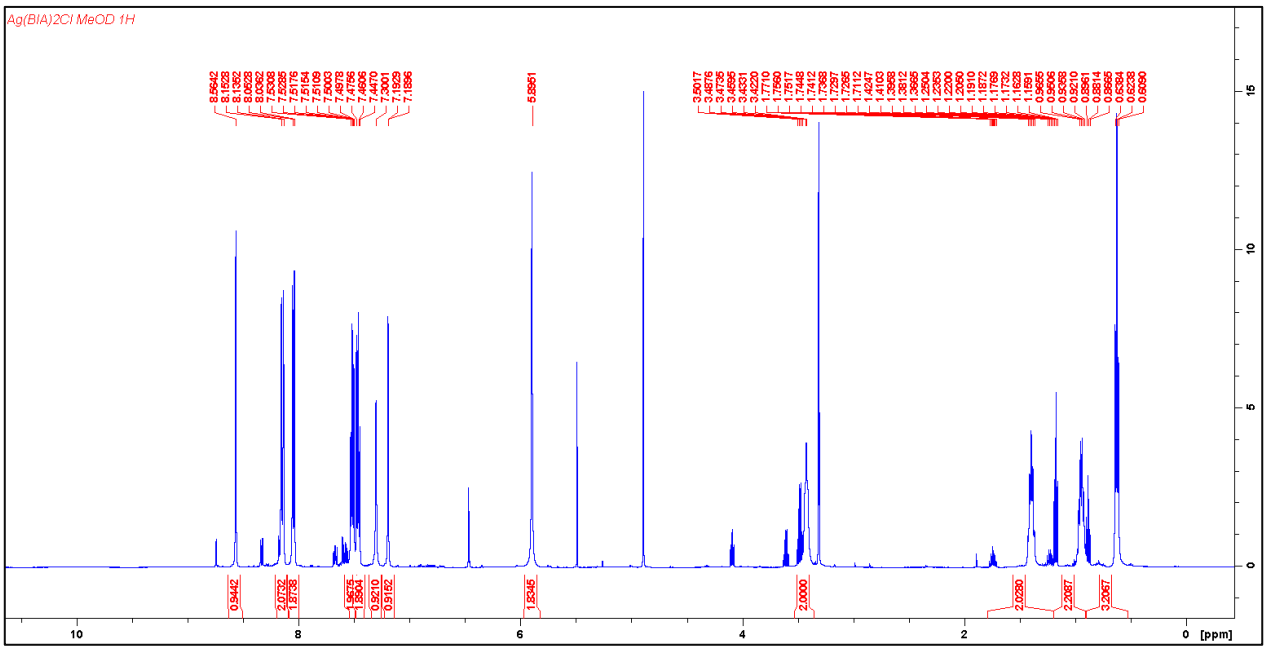

Figure S4 Bis(1-(anthracen-9-ylmethyl)-3- butylimidazol-2-ylidene) silver chloride $[Ag(BIA)_2]Cl$ **(2)**, ^{1}H NMR

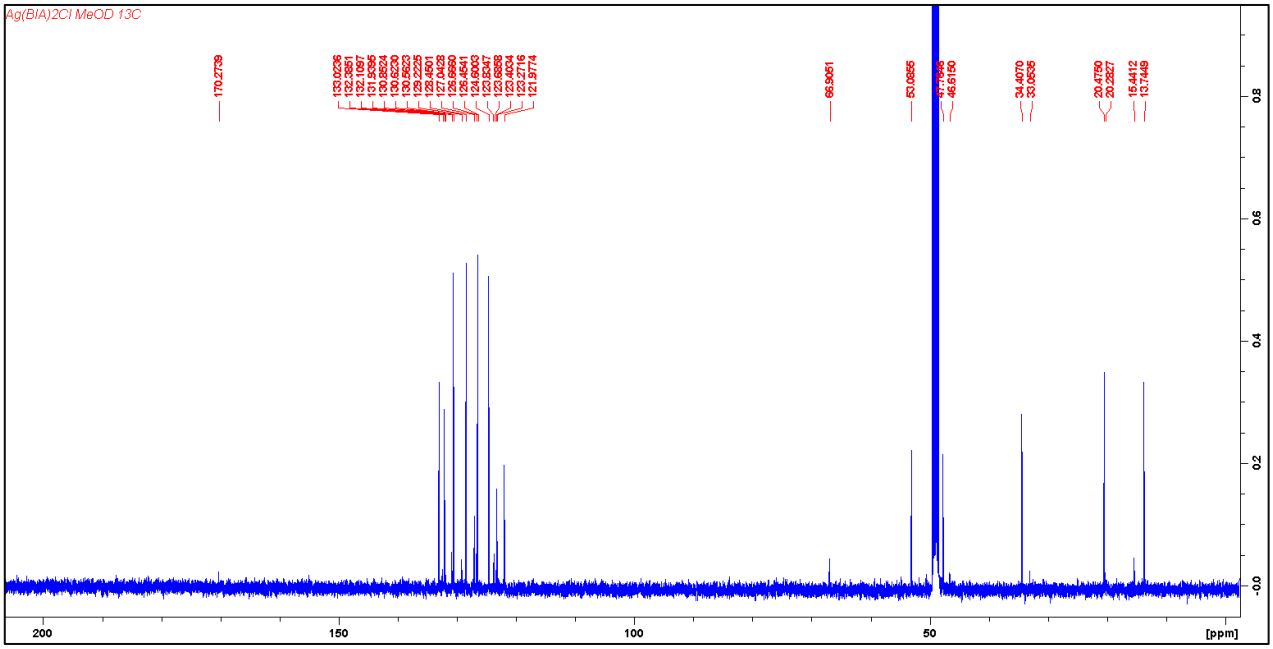

Figure S5 Bis(1-(anthracen-9-ylmethyl)-3- butylimidazol-2-ylidene) silver chloride $[Ag(BIA)_2]Cl$ **(2)**, ^{13}C NMR

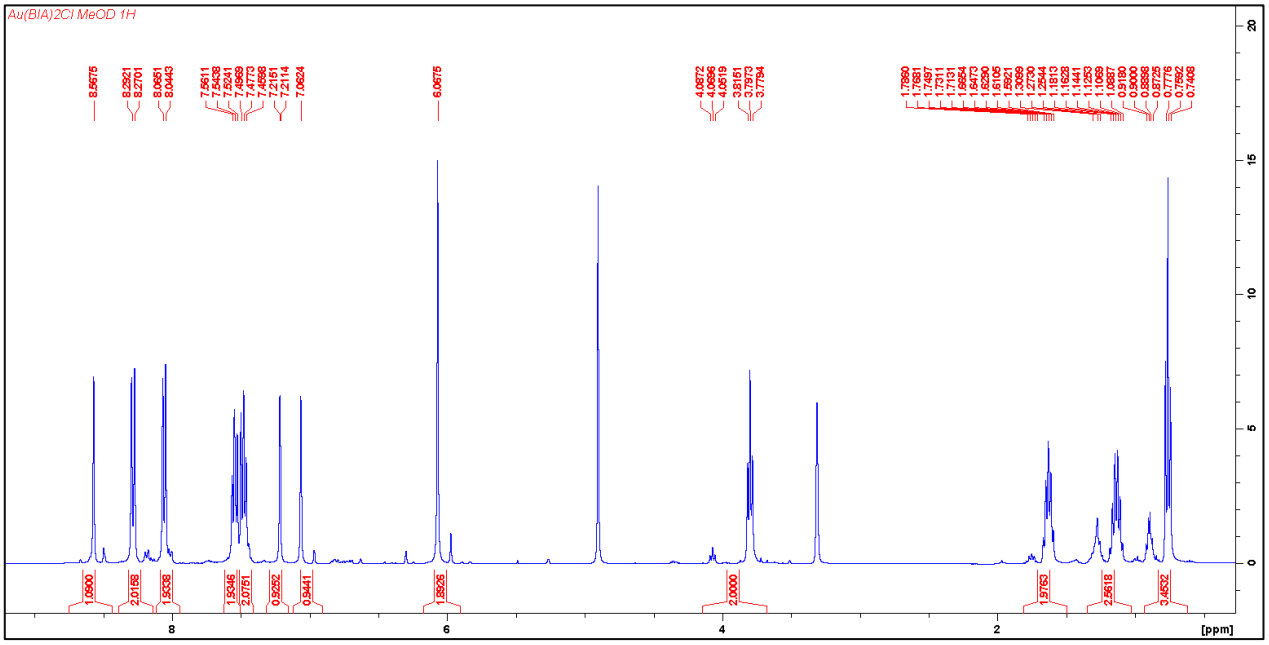

Figure S6 Bis(1-(anthracen-9-ylmethyl)-3- butylimidazol-2-ylidene) gold chloride $[Au(BIA)_2]Cl$ **(3)**, ^{1}H NMR

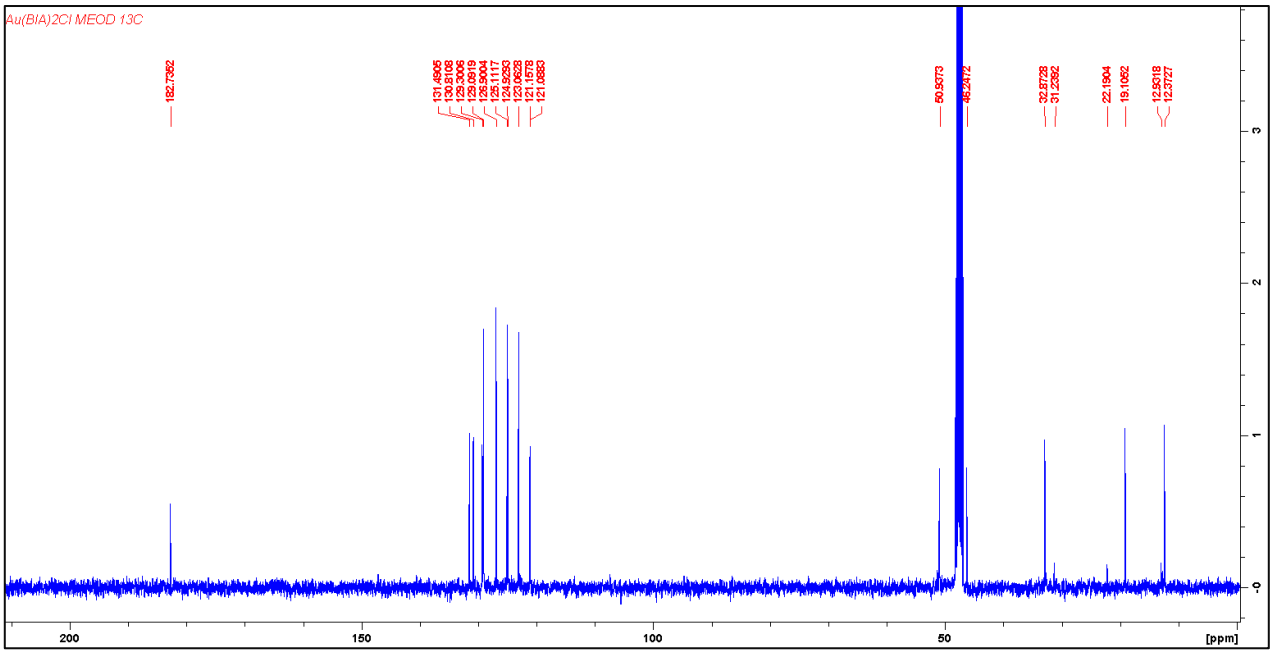

Figure S7 Bis(1-(anthracen-9-ylmethyl)-3- butylimidazol-2-ylidene) gold chloride $[Au(BIA)_2]Cl$ **(3)**, ^{13}C NMR

Stability and solubility in aqueous solution

To verify the stability of $[Ag(BIA)_2]Cl$ and $[Au(BIA)_2]Cl$ complexes in a buffer solution (NaCl 0.1 M, NaCac 2.5 mM, pH = 7.0, T = 25.0 °C) a UV spectrum was recorded every 10 minutes from 0 to 3 hours, mixing the solution before recording the spectrum. Three hours is a time range in line with the time needed for our experiments. The silver compound is stable (Figure S8); differently, as shown in Figure S9, the gold complex profile is not fully reproducible, with a change in the spectral profile that suggests some aggregation process on the cell walls; in fact, the peaks at 256 nm and 273 nm switch their prevalence as time goes by, despite mixing.

This hypothesis is confirmed by spectra registered at an increasing temperature in the 25.0 - 90.0 °C range (one every 5.0 °C). The silver complex undergoes limited variations confirming sufficient stability (Figure S10); in the gold complex (Figure S11), the spectra undergo more significant changes but with the maximum at 274 nm always remaining the main one at the highest temperatures and thus discarding degradation processes. These lower stability issues, in some cases, prevented performing with the gold complex the same detailed study done with silver; on the other hand, the experiments below still enabled us to compare the features driven by the two different metal centres.

In the case of the silver compound, absorption measurements were performed also by varying the metal complex concentration to verify the linearity of the Lambert-Beer in the working concentration range; this was respected at all the wavelengths (Figure S12A). To assess whether aggregation phenomena are at play, we can emphasize any deviations from linearity by evaluating the ratio between two wavelengths. In the absence of aggregation, the ratio should be constant: Figure S12B shows that the silver complex does not undergo auto-aggregation.

The analysed metal complexes contain an anthracenyl residue, which is fluorescent. Only the silver complex showed a stable fluorescence signal in solution; the emission spectrum of $[Ag(BIA)_2]^+$ recorded at λ_{ex} = 368 nm shows emission maxima at 392 nm, 415 nm, and 438 nm (Figure S13).

Fluorescence emission spectra of $[Ag(BIA)_2]^+$ were also done by varying the complex concentration to verify the linearity between concentration and fluorescence signal (Figure S14). Linearity is respected in the investigated concentration range (C_{Ag} from 0.649 nM to 0.352 µM).

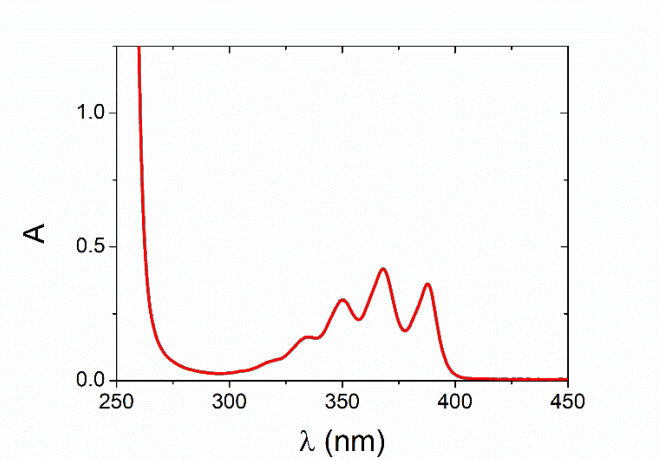

Figure S8 Spectra of $[Ag(BIA)_2]^+$ in aqueous solution (C_{Ag} = 22.0 µM) recorded during the time. The spectra are done every 10 min from 0 (black line) to 3 (red line) hours, mixing every time before recording the spectrum. NaCl 0.1 M, NaCac 2.5 mM, pH = 7.0, T = 25.0 °C.

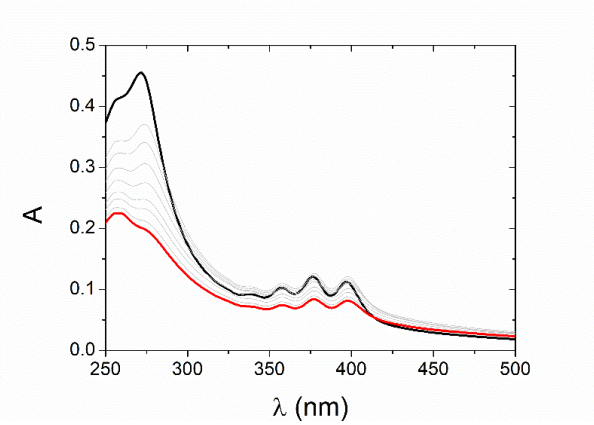

Figure S9 Spectra of $[Au(BIA)_2]^+$ in aqueous solution (C_{Au} = 6.55 µM) recorded during the time. The spectra are done every 20 min from 0 (black line) to 3 (red line) hours, mixing every time before recording the spectrum. NaCl 0.1 M, NaCac 2.5 mM, pH = 7.0, T = 25.0 °C.

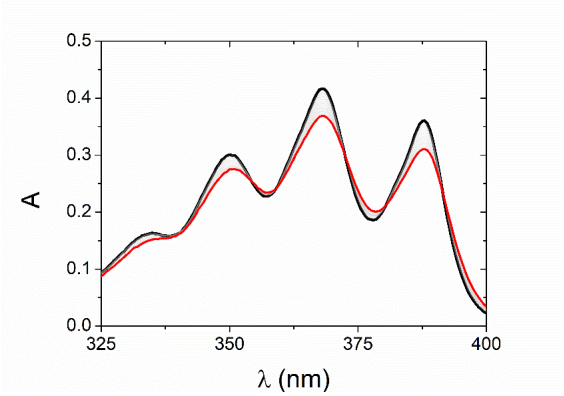

Figure S10 Spectra of $[Ag(BIA)_2]^+$ in aqueous solution (C_{Ag} = 22.0 µM) at different temperatures (one spectrum every 5.0 °C) from 25 °C (black line) to 90 °C (red line). NaCl 0.1 M, NaCac 2.5 mM, pH = 7.0.

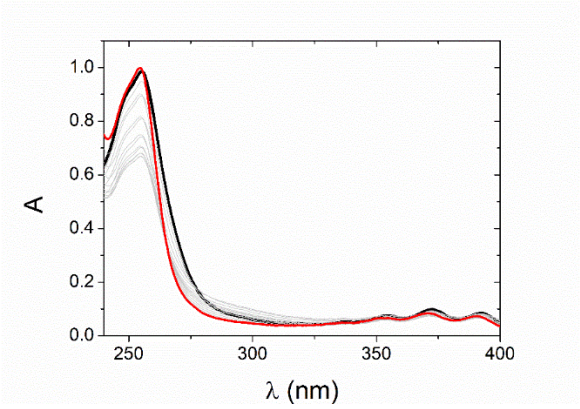

Figure S11 Spectra of $[Au(BIA)_2]^+$ in aqueous solution (C_{Au} = 10.9 µM) at different temperatures (one spectrum every 5.0 °C) from 25 °C (black line) to 90 °C (red line). NaCac 2.5 mM, pH = 7.0.

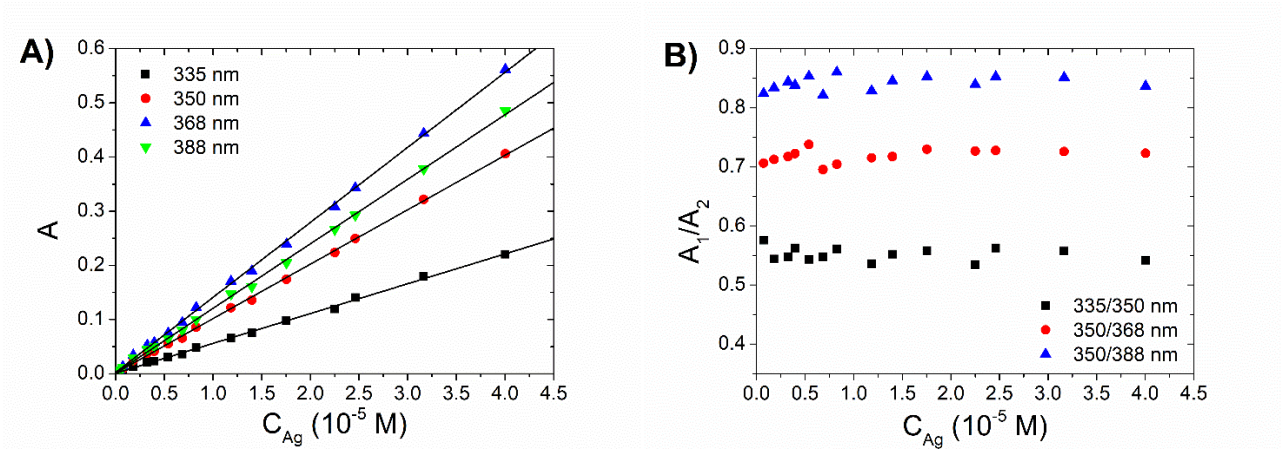

Figure S12 On the left, absorbance at a different wavelength at the increasing amount of $[Ag(BIA)_2]^+$. On the right, the ratio of two different absorbances A_1/A_2 as a function of the concentration of $[Ag(BIA)_2]^+$. NaCl 0.1 M, NaCac 2.5 mM, pH = 7.0, T = 25.0 °C.

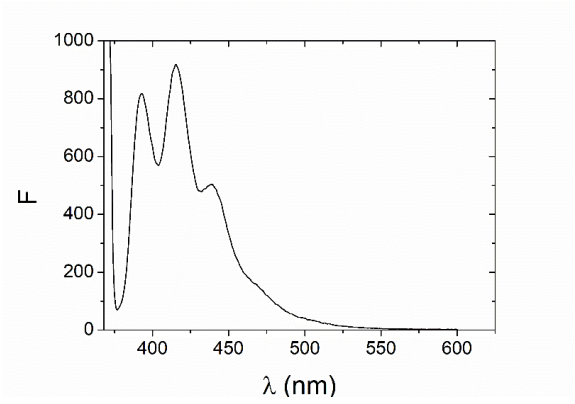

Figure S13 Emission spectrum of $[Ag(BIA)_2]^+$. C_{Ag} = 0.216 µM, NaCl 0.1 M, NaCac 2.5 mM, pH = 7.0, T = 25.0°C, λ_{ex} = 368 nm, slit 5 nm.

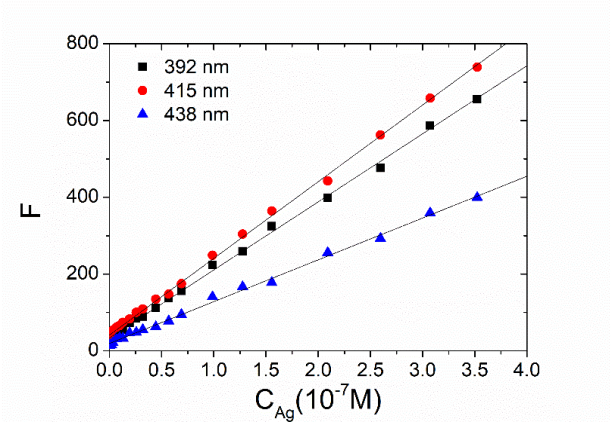

Figure S14 Fluorescence intensities at different wavelengths for increasing amounts of $[Ag(BIA)_2]^+$. NaCl 0.1 M, NaCac 2.5 mM, pH = 7.0, T = 25.0 °C, λ_{ex} = 368 nm, slit 5 nm.

Cellular tests

Cytotoxicity

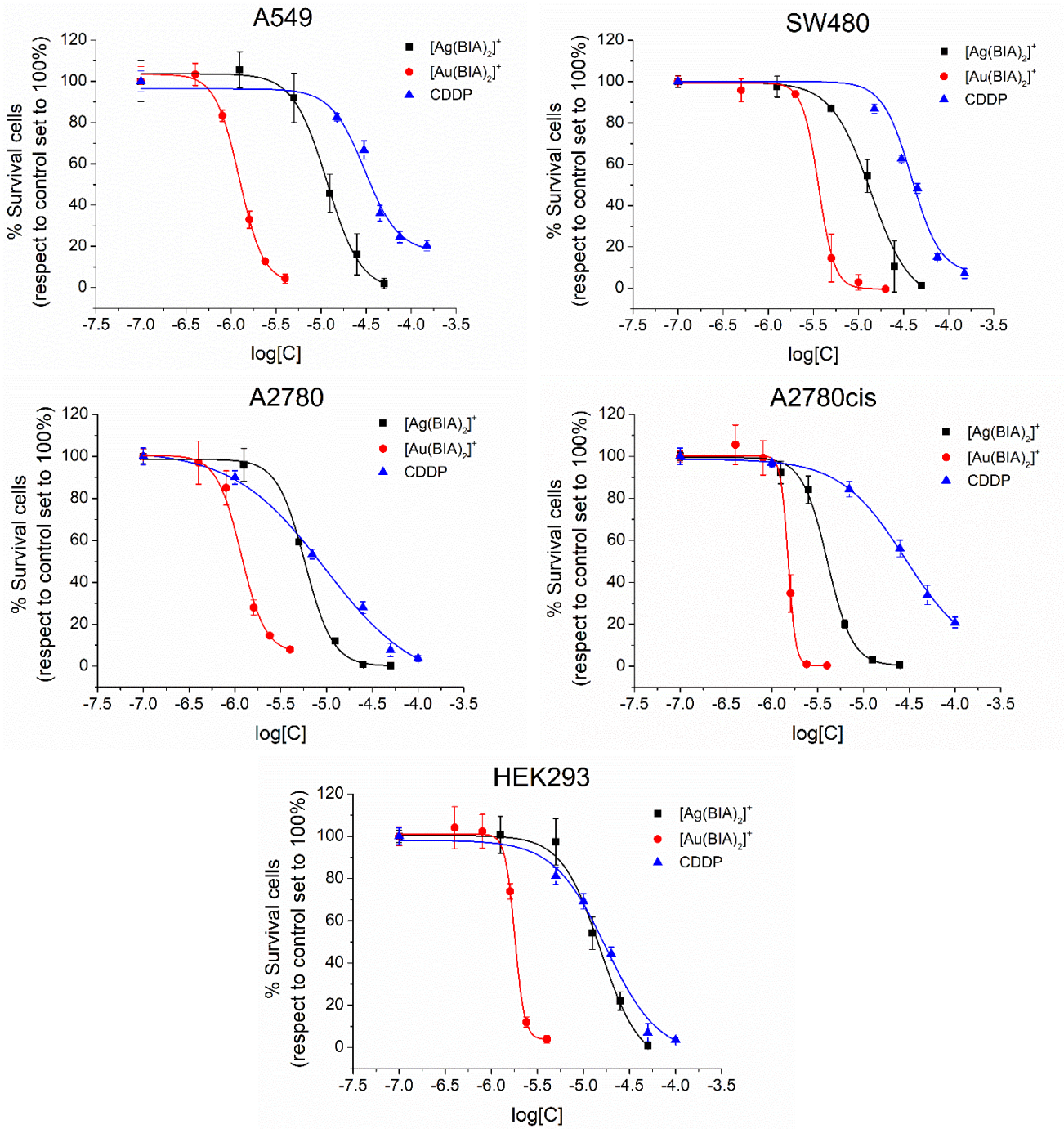

Figure S15 Percentage of surviving cells as a function of $[Ag(BIA)_2]^+$, $[Au(BIA)_2]^+$, and CDDP concentration on A549, SW480, A2780, A2780cis and HEK293 cell lines.

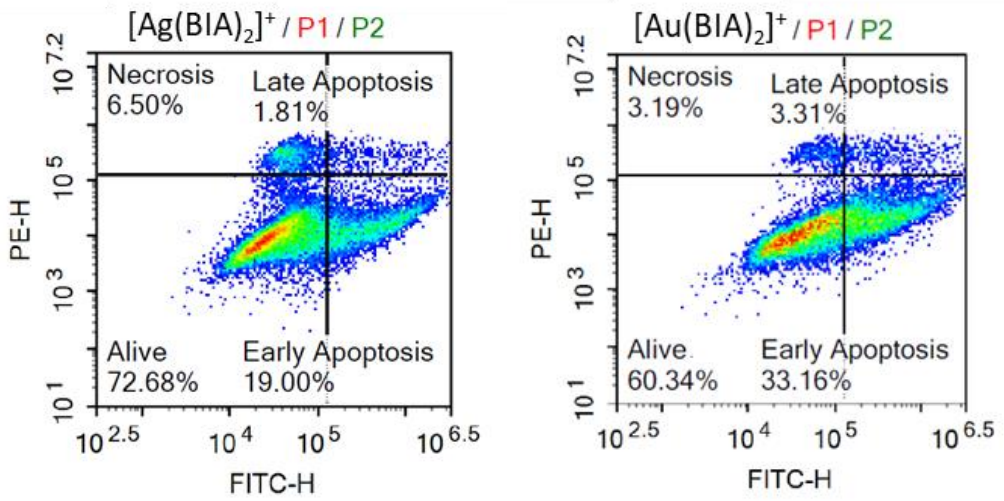

Figure S16 Annexin V-FITC/PI double staining. Screenshots of the software outcome based on a NovoCyte Flow cytometer experiment analysed by using the NovoExpress 1.4.0 Software.

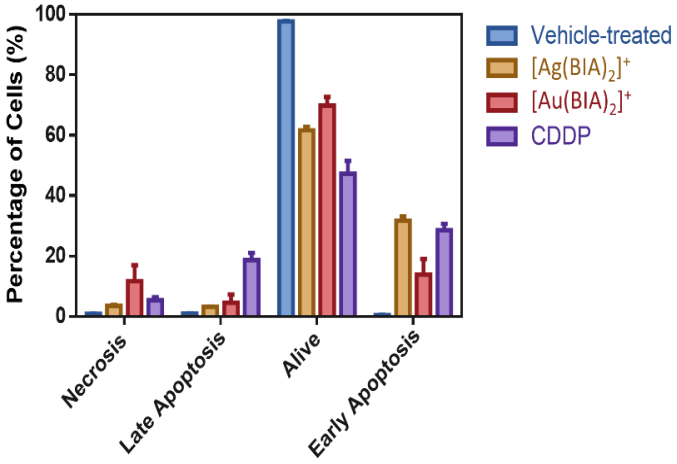

Figure S17 Flow cytometry of human lung carcinoma cells (A549) with 24h of incubation, treated at the IC_{50} concentration of the complex. Error bars are the standard deviations over all the measured samples in two different experiments.

Cellular uptake and $logP_{o/w}$

Table S1 Cellular uptake expressed as µmol of metal (M) in 10^6 cells, after 24 h of incubation at 37 °C. $logP_{o/w}$ = $log([complex]_o / [complex]_w)$, M = Ag, Au, or Pt.

	µmol M/cells (10^{-6})	$logP_{o/w}$
$[Ag(BIA)_2]^+$	51 ± 2	1.0
$[Au(BIA)_2]^+$	52.3 ± 0.5	1.8
CDDP	26 ± 2	-2.4

BSA interaction

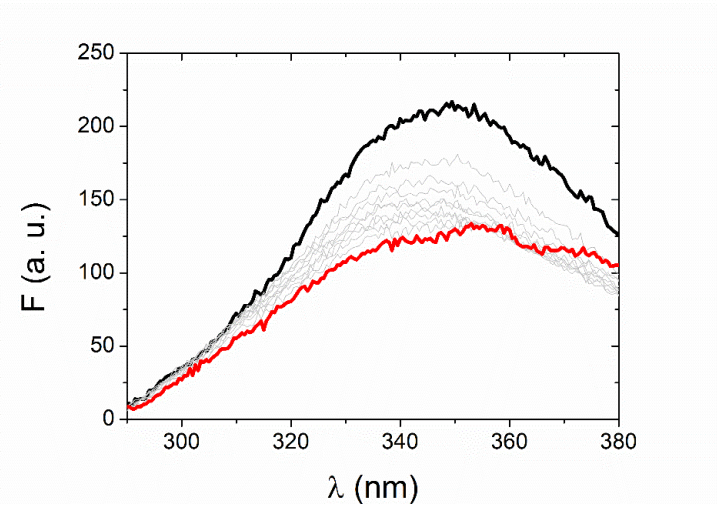

Figure S18 Fluorescence spectra, corrected for dilution, of BSA in the presence of increasing amounts of $[Ag(BIA)_2]^+$; C_{BSA} 1.03 µM, $C_{[Ag(BIA)2]+}$ from 0 M (black line) to 19.6 µM (red line); NaCl 0.1 M NaCac 2.5 mM, pH = 7.0, T = 25.0 °C; slits 3 nm.

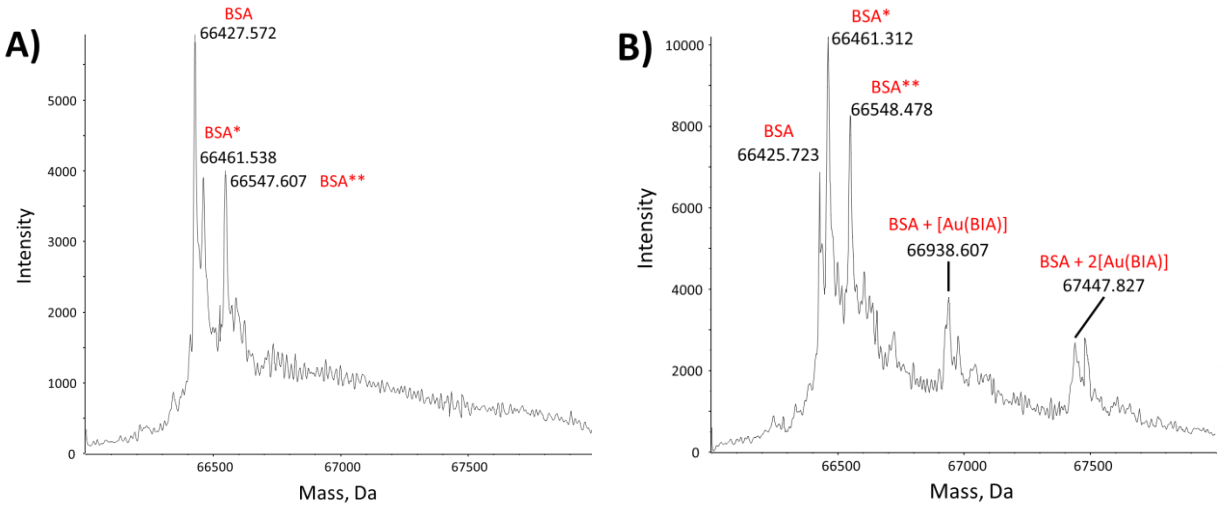

Figure S19 Deconvoluted mass spectra of BSA alone (A), C_{BSA} = 1.00 µM, in presence of 2.00 µM of $[Au(BIA)_2]^+$ (B) in NH_4OAc solution 20 mM, pH = 6.8, 0.1% v/v of formic acid has been added just before injection into the mass spectrometer. BSA* = sulfinilation on Cys34; BSA** = cysteinylation on Cys34.

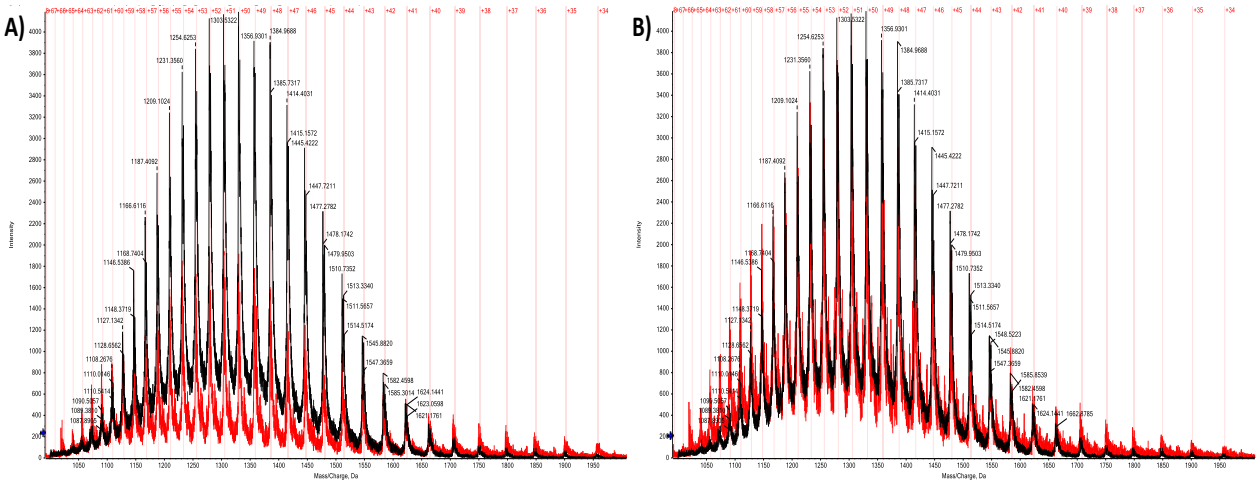

Figure S20 Protonation state of the BSA alone (black line) and (A) $[Ag(BIA)_2]^+$/BSA system (red line) or (B) $[Au(BIA)_2]^+$/BSA system (red line).

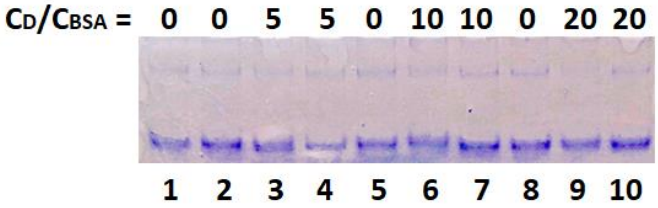

Figure S21 Native acrylamide electrophoresis of BSA incubated overnight with $[Au(BIA)_2]^+$ and $[Ag(BIA)_2]^+$ complexes at 37.0 °C. C_{BSA} = 2 μM, C_D = 10, 20 and 40 μM. Buffer NaCl 0.1 M, NaCac 2.5 mM, pH 7.0. **1)** BSA alone; **2, 5, 8)** BSA with 0.075%, 0.15%, and 0.3% of DMSO; **3, 6, 9)** BSA with $[Au(BIA)_2]^+$, C_D/C_{BSA} = 5.0, 10, 20; **4, 7, 10)** BSA with $[Ag(BIA)_2]^+$, C_D/C_{BSA} = 5.0, 10, 20.

Table S2 Equilibrium constants for $[Ag(BIA)_2]^+$/BSA at different temperatures; 0.1 M NaCl, 2.5 mM NaCac, pH = 7.0.

T (°C)	K_{BSA} (10^6 M^{-1})
15.0	0.50 ± 0.03
25.0	1.92 ± 0.07
37.0	2.9 ± 0.1
48.0	8.3 ± 0.6

Table S3 Equilibrium constants for the marker+BSA exchange titrations with $[Ag(BIA)_2]^+$; 0.1 M NaCl, 2.5 mM NaCac, pH = 7.0, T = 25.0 ° C.

	Site	K_{BSA} (10^5 M^{-1})
BSA		19.2 ± 0.7
Phenylbutazone	I	12 ± 1
Ibuprofen	II	5.8 ± 0.3

DNA/RNA interaction

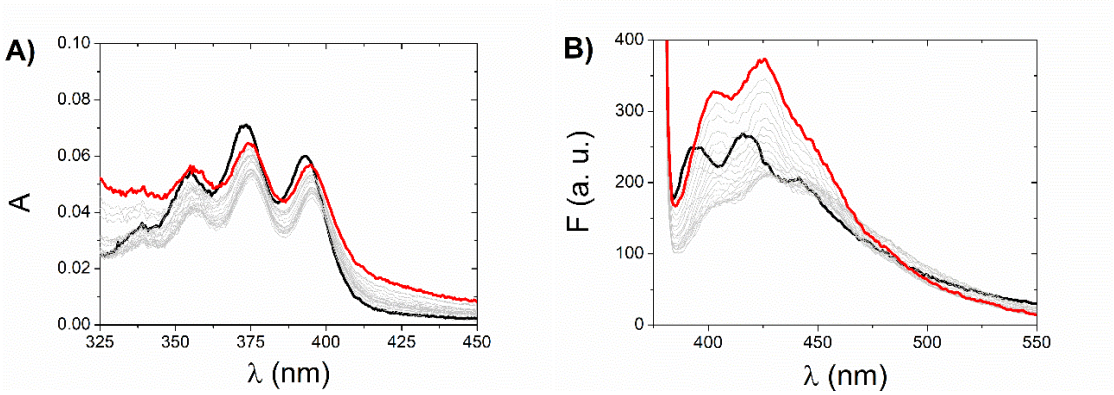

Figure S22 (A) Absorbance spectra corrected for dilution of $[Au(BIA)_2]^+$ (C_{Au} = 8.73 µM) at increasing amount of DNA from 0 (black line) to 463 µM (red line). (B) Emission spectra (λ_{ex} = 374 nm, slit 5 nm) corrected for dilution of $[Au(BIA)_2]^+$ (C_{Au} = 7.23 µM) at increasing amount of DNA from 0 (black line) to 713 µM (red line). NaCac 2.5 mM, pH = 7.0, T = 25.0 °C; DNA concentration in base pairs.

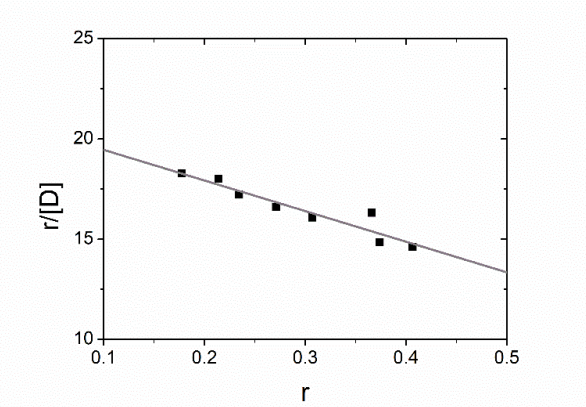

Figure S23 Scatchard plot for the $[Ag(BIA)_2]^+$/DNA system. C_{Ag} = 16.9 µM, NaCl 0.1 M, NaCac 2.5 mM, pH = 7.0, T = 25.0 °C. The Scatchard equation is as follows:

$$\frac{r}{[D]} = BK_{SC} - K_{SC}r$$

where r = [PD]/C_P, P is the polynucleotide base pair, D is the metal complex, PD is the metal complex/DNA adduct, [D] = C_D – [PD] and [PD] = $\Delta A/\Delta\varepsilon$, $\Delta\varepsilon = \varepsilon_{PD} - \varepsilon_D$ being ε_i the molar extinction coefficient of the i-th species, K_{SC} is the Scatchard equilibrium constant and B is a parameter connected to the site size, n (n = (1+1/B)/2). A plot of r/[D] over r yields K_{SC} = 1.53×10^4 M^{-1}, $K_{SC}B$ = 2.10×10^4 M^{-1} ($\log K_{SC}B$ = 4.3), B = 1.37, n = 0.86.

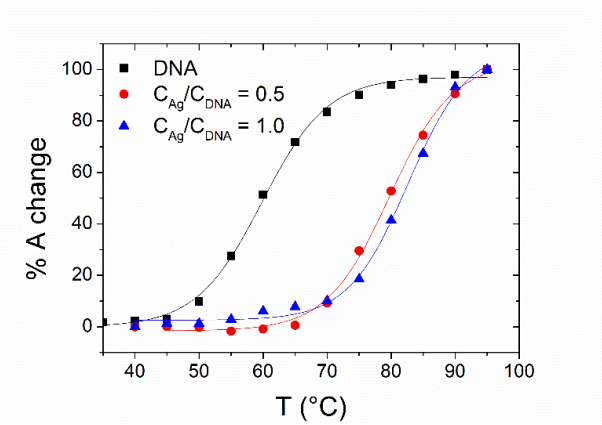

Figure S24 Absorption (260 nm) as a function of temperature of DNA alone (C_{DNA} = 20.0 µM) and in the presence of the metal complex $[Ag(BIA)_2]^+$ in the ratio $C_{[Ag(BIA)2]+}/C_{DNA}$ equal to 0.5 or 1.0, in buffer solution 2.5 mM NaCac, pH = 7.0.

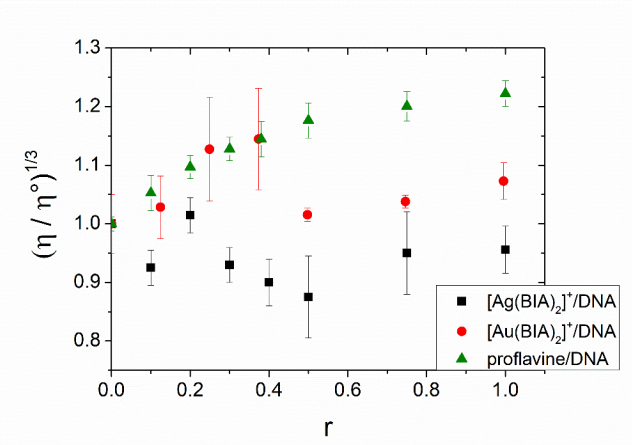

Figure S25 Relative viscosity plot for the $[Ag(BIA)_2]^+$/DNA (black square) or $[Au(BIA)_2]^+$/DNA (red circles) systems as a function of the ratio r = C_D/C_{DNA}; C_{DNA} = 118 μM; NaCl 0.1 M, NaCac 2.5 mM, pH 7.0, T = 25.0 °C; DNA concentration in base pairs. The green triangles represent the results obtained in the case of the intercalator Proflavine.

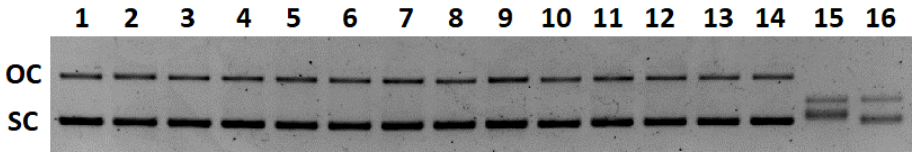

Figure S26 Electrophoresis mobility assay after 24 h of incubation at 37.0 °C of **1** and **8)** pUC18 (6.52 μM base pairs) alone; **2** and **9**) with the max % of DMSO used; **3-7**) $[Au(BIA)_2]^+$ in a ratio C_{Au} / C_{pUC18} = 0.1, 0.2, 0.3, 0.4, 0.5; **10-14**) $[Ag(BIA)_2]^+$ in a ratio C_{Ag} / C_{pUC18} = 1.0, 2.0, 4.6, 6.4, 8.5; **15-16**) CDDP in a ratio C_{Pt} / C_{pUC18} = 1.0, 2.0. NaCac 2.5 mM, pH = 7.0.

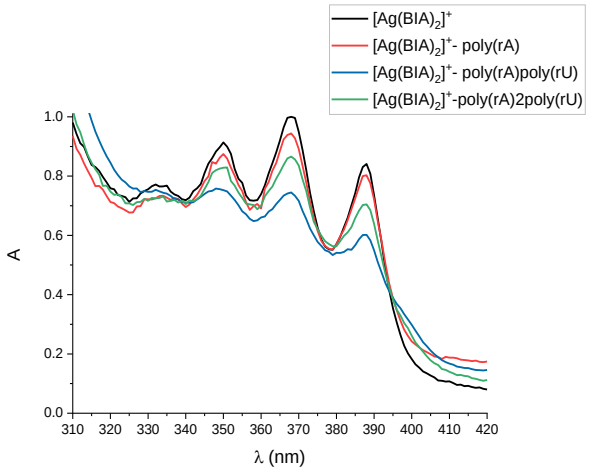

Figure S27 Comparison of absorption spectra of $[Ag(BIA)_2]^+$ alone (C_{Ag} = 16.9 μM) and in the presence of RNA in single (poly(rA)), double (poly(rA)poly(rU)), and triple (poly(rA)2poly(rU)) helix; complex:nucleic acid = 1:3 with nucleic acid expressed as phosphate groups, base pairs or base triplets respectively; NaCac 2.5 mM, pH = 7.0, T = 25.0 °C.

Table S4 Equilibrium constants from absorbance and fluorescence titrations calculated with different equations and methods for the $[Ag(BIA)_2]^+$/DNA system at different concentrations of NaCl, NaCac 2.5 mM, pH = 7.0, T = 25.0 °C.

		ABSORBANCE log K_{DNA}		
- log [Na^+]	**Eq (1)**	**Eq (2)**	**HypSpec® n = 1**	**HypSpec® n = 2**
2.60	4.920 ± 0.005	4.950 ± 0.005	4.61 ± 0.05	5.04 ± 0.05
2.30	4.800 ± 0.005	4.77 ± 0.01	4.54 ± 0.02	4.97 ± 0.03
1.76	4.490 ± 0.005	4.470 ± 0.005	4.39 ± 0.01	4.780 ± 0.005
1.24	4.220 ± 0.005	4.200 ± 0.005	4.170 ± 0.005	4.530 ± 0.005
0.99	4.09 ± 0.01	4.030 ± 0.005	3.97 ± 0.01	4.31 ± 0.01
		FLUORESCENCE log K_{DNA}		
- log [Na^+]	**Eq (1)**	**Eq (2)**	**HypSpec® n = 1**	**HypSpec® n = 2**
2.60	5.610 ± 0.005	5.650 ± 0.005	5.52 ± 0.05	5.83 ± 0.05
2.30	5.420 ± 0.005	5.48 ± 0.02	5.35 ± 0.10	5.65 ± 0.10
1.76	5.050 ± 0.005	5.08 ± 0.01	4.98 ± 0.10	5.28 ± 0.10
1.24	4.520 ± 0.005	4.510 ± 0.005	4.50 ± 0.05	4.80 ± 0.05
0.99	4.30 ± 0.02	4.300 ± 0.005	4.23 ± 0.03	4.53 ± 0.03

Table S5 Melting temperature (T_m) values for CT-DNA (C_{DNA} = 20.0 μM) alone and in the presence of the $[Ag(BIA)_2]^+$ metal complex; $\Delta T_m = T_m$ ($[Ag(BIA)_2]^+$/DNA) - T_m (DNA); 2.5 mM NaCac, pH 7.0; DNA concentration in base pairs.

$C_{[Ag(BIA)2]+}/C_{DNA}$	T_m (°C)	ΔT_m (°C)
0.0	59.8 ± 0.3	–
0.5	79.8 ± 0.4	20.0 ± 0.7
1.0	82.6 ± 0.5	22.8 ± 0.8

Table S6 Melting temperature (T_m) values for double helix RNA alone (C_{AU} = 20.2 μM) and in the presence of an equal amount of complex $[Ag(BIA)_2]^+$; all buffers also contain NaCac 2.5 mm, pH = 7.0; RNA concentration in base pairs.

C_{NaCl} (M)	T_m (°C) poly(rA)poly(rU)	T_m (°C) $[Ag(BIA)_2]^+$/poly(rA)poly(rU)	ΔT_m (°C)
0	43.6 ± 0.5	48.0 ± 1.0	4.4 ± 1.5
0.007	42.2 ± 0.3	44.1 ± 0.6	1.9 ± 0.9
0.100	56.3 ± 0.3	52.8 ± 0.5	-3.5 ± 0.8

G-quadruplexes

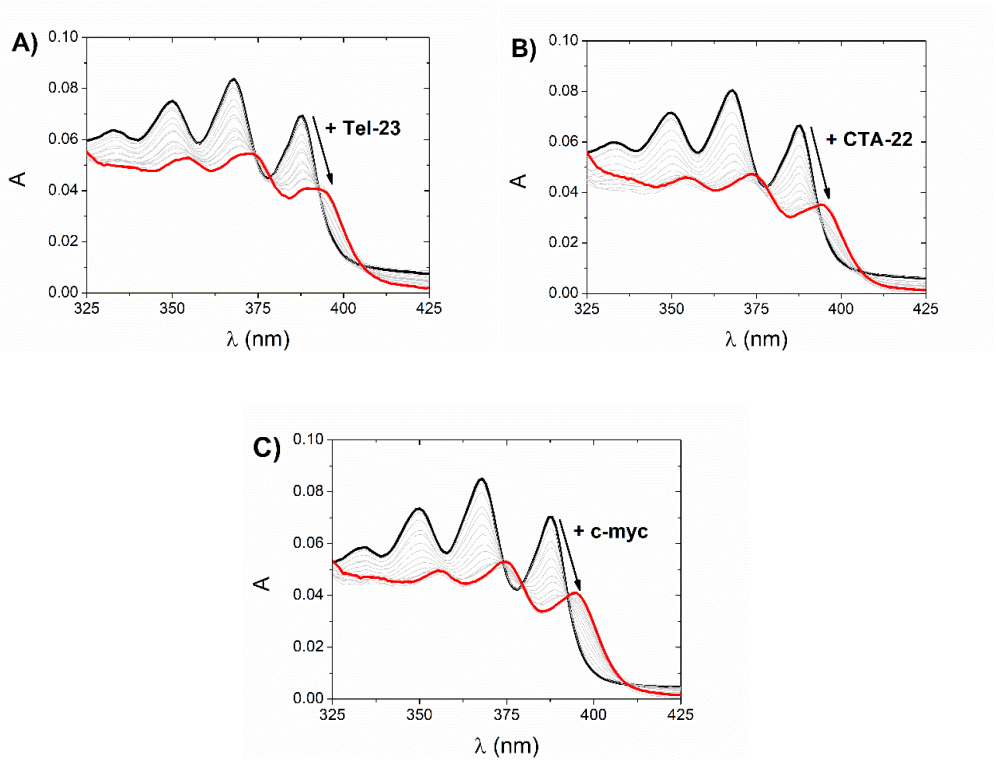

Figure S28 Absorbance spectra of $[Ag(BIA)_2]^+$ (corrected by dilution), at increasing amounts of A) Tel-23 from 0 to 63.2 µM; B) CTA-22 from 0 to 55.4 µM; C) c-myc from 0 to 53.5 µM. C_{Ag} = 16.9 µM, KCl 0.1 M, LiCac 2.5 mM, pH = 7.0, T = 25.0 °C.

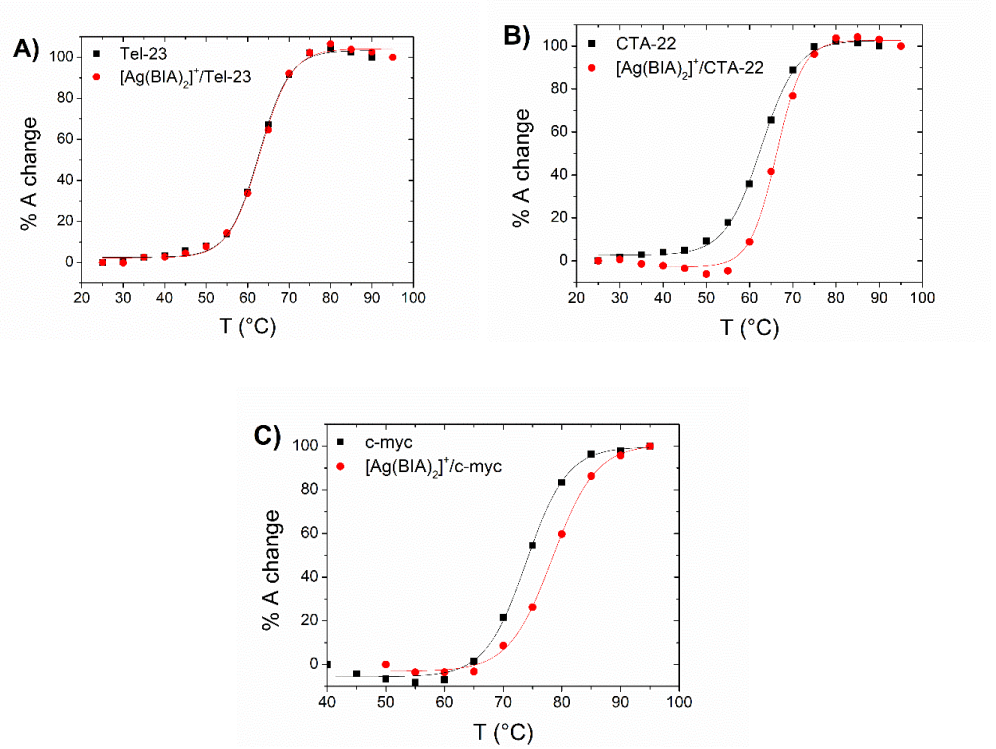

Figure S29 Melting curves for the G4 alone and metal complex/G4 mixtures. A) Tel-23 and $[Ag(BIA)_2]^+$/Tel-23; B) CTA-22 and $[Ag(BIA)_2]^+$/CTA-22; C) c-myc and $[Ag(BIA)_2]^+$/c-myc. C_{G4} = 25.0 µM (in strands), [complex]/[G4] = 0.5. KCl 0.1 M, LiCac 2.5 mM, pH = 7.0 for Tel23 and CTA22 (KCl 0.01 M for c-myc). This difference is needed as the c-myc is very stable and a higher concentration of KCl would stabilise so much that the structure would have a denaturation temperature out of the detection window.

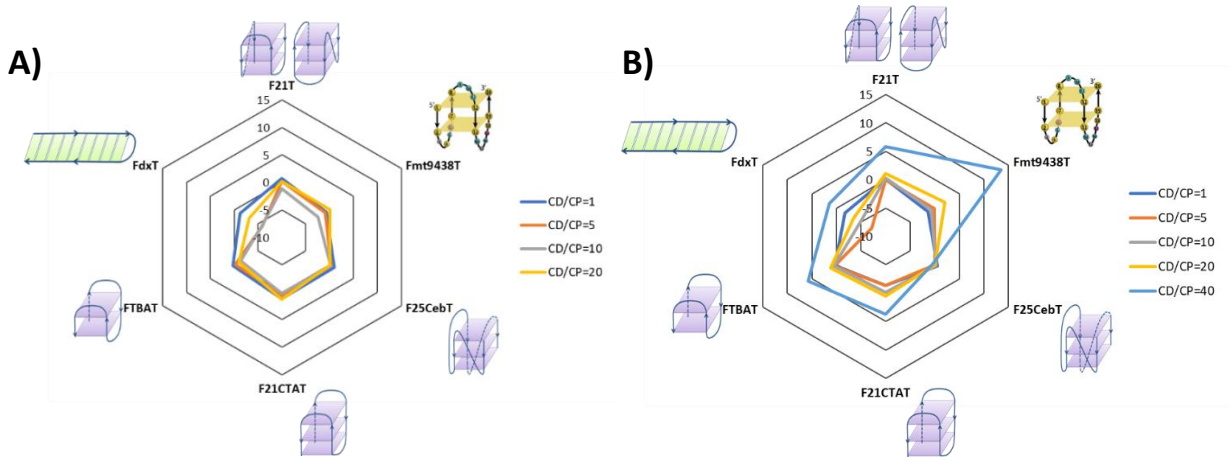

Figure S30 Spider plot of FRET melting of P = polynucleotide, and D = metal complex, where C_P = 0.2 µM (in strands), of the systems: A) $[Ag(BIA)_2]^+$/P with C_D/C_p = 1.0, 5.0, 10, and 20; B) $[Au(BIA)_2]^+$/P with C_D/C_p = 1.0, 5.0, 10, 20 and 40. KCl 10 mM, LiCl 90 mM, LiCac10 mM, pH = 7.0.

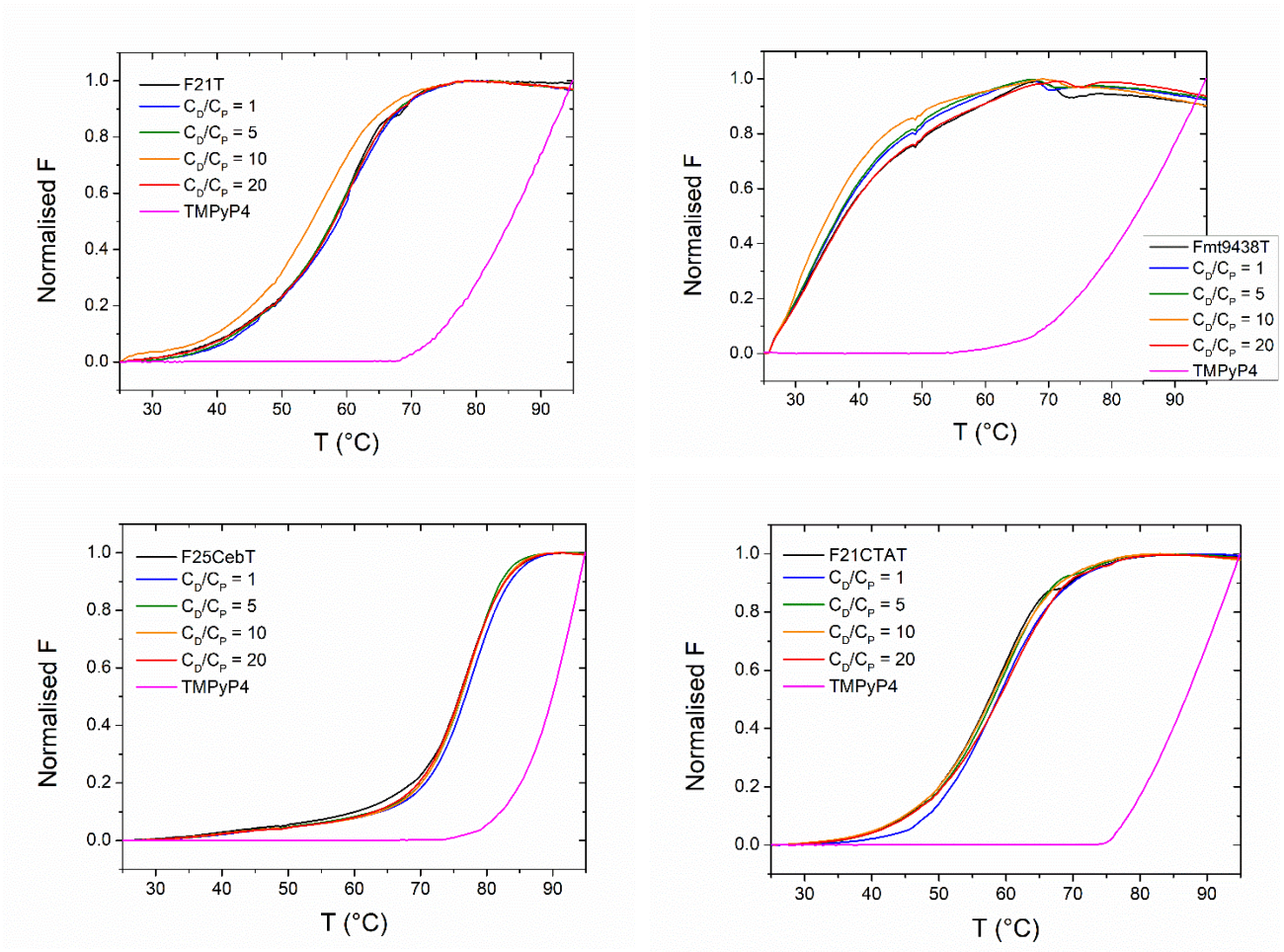

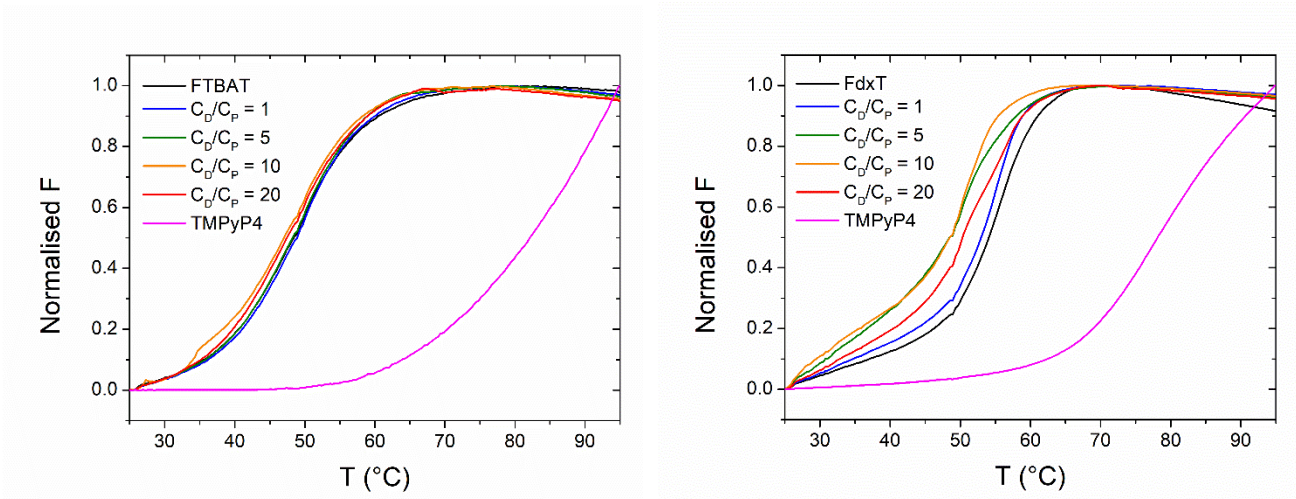

Figure S31 Normalised FRET melting profile of P = polynucleotide, and D = metal complex, where C_P = 0.2 µM (in strands), of the systems $[Ag(BIA)_2]^+$/P of Figure S30A. TMPyP4 is used as positive control at C = 2.0 µM. KCl 10 mM, LiCl 90 mM, LiCac10 mM, pH = 7.0. The data are the one of a single experiment but final values of Figure S29A are the mean of four experiments.

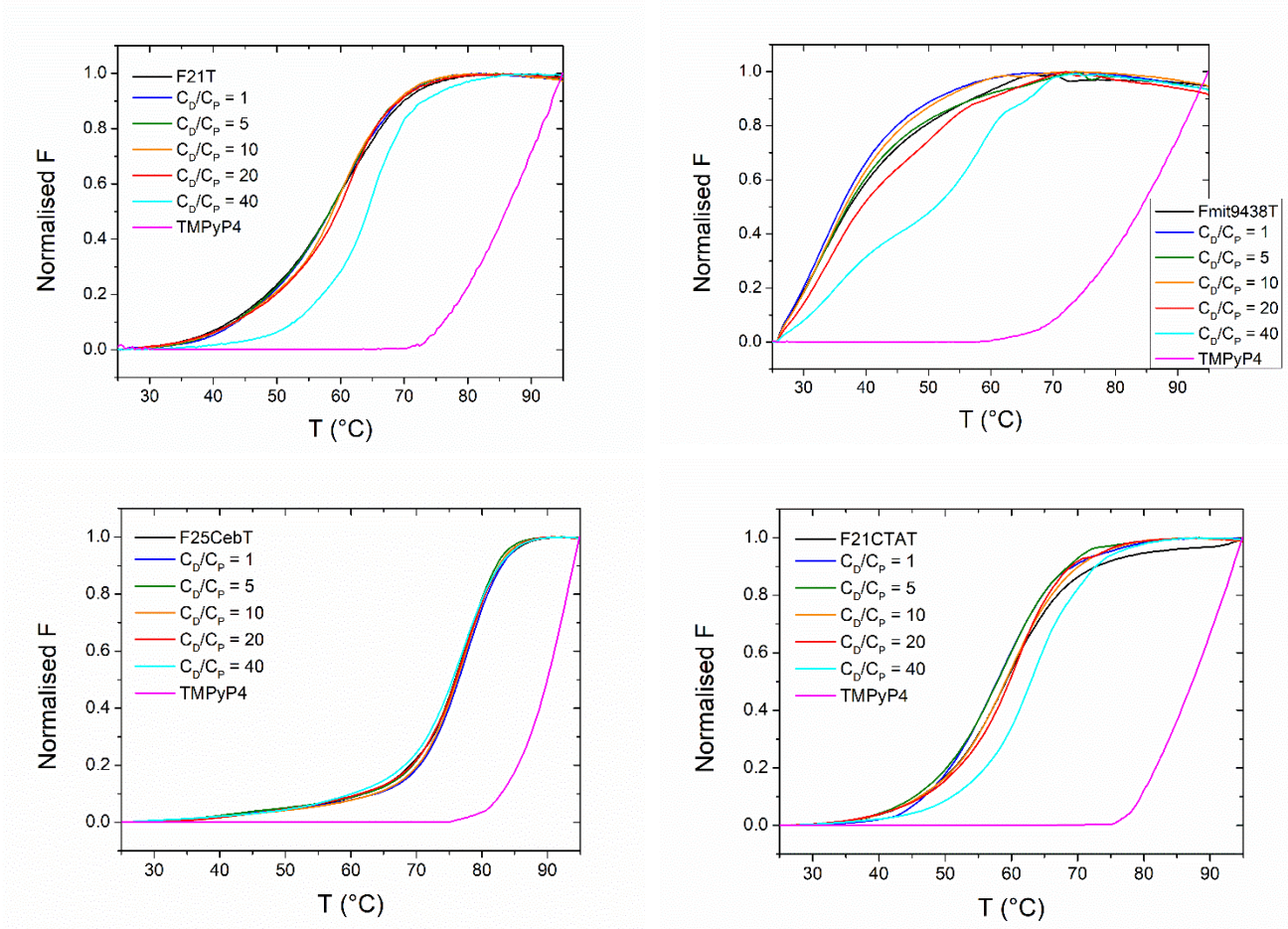

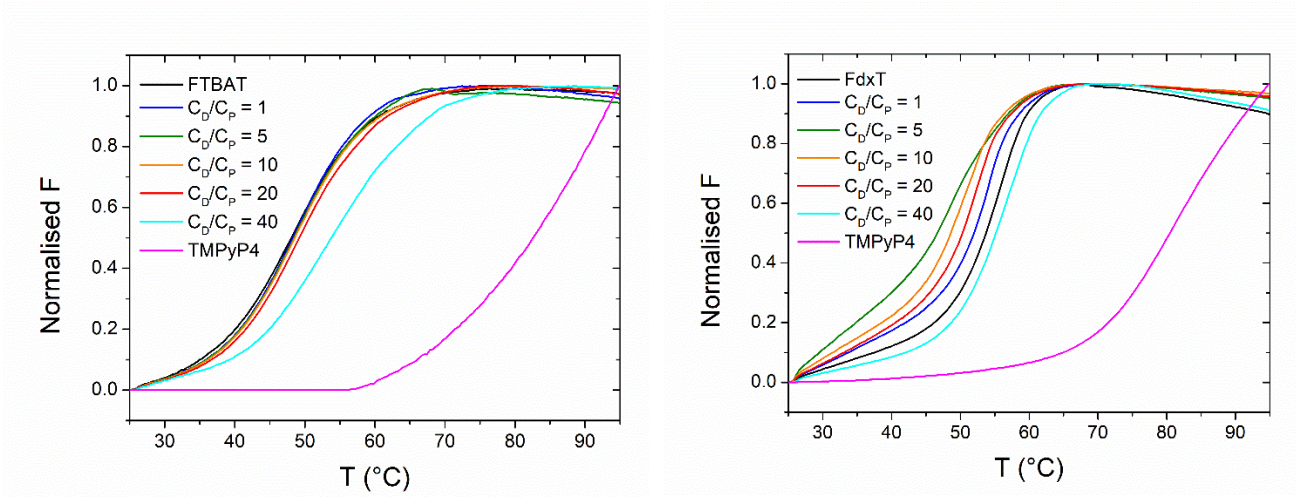

Figure S32 Normalised FRET melting profile of P = polynucleotide, and D = metal complex, where C_P = 0.2 μM (in strands), of the systems $[Au(BIA)_2]^+$/P of Figure S30B. TMPyP4 is used as positive control at C = 2.0 μM. KCl 10 mM, LiCl 90 mM, LiCac10 mM, pH = 7.0. The data are the one of a single experiment but final values of Figure S29B are the mean of four experiments.

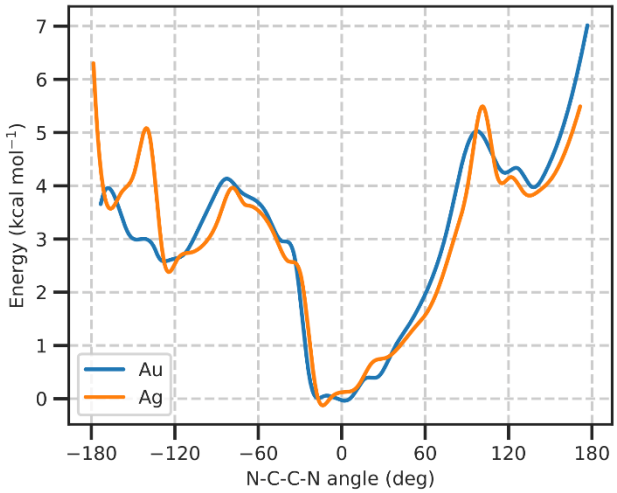

Figure S33 Relaxed scans of the N-C-C-N dihedral angle for both the Ag and Au complexes.

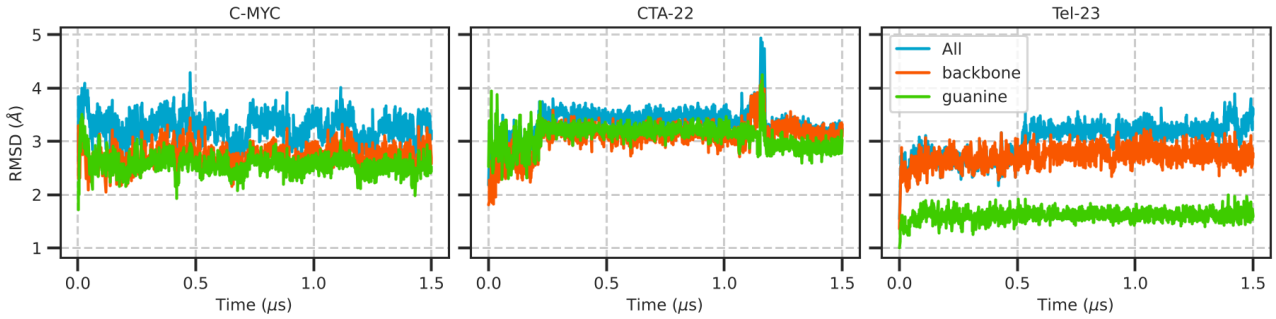

Figure S34 RMSD computed along the MM MD for the three targets.

Table S7 Lowest binding energy (ΔG), in kcal mol^{-1}, for the two metal complexes docked in Tel-23, CTA-22, and c-myc G-quadruplexes. The lowest docking binding energy (kcal mol^{-1}), the stronger the ligand-target interaction.

	Tel-23	**CTA-22**	**c-myc**
$[Ag(BIA)_2]^+$	-2.64	-2.81	-3.17
$[Au(BIA)_2]^+$	-3.02	-3.01	-2.72

Table S8 Spectral characteristics and bathochromic shift of absorption maxima of the $[Ag(BIA)_2]^+$ complex following the interaction with G4 of different conformations; KCl 0.1 M LiCac 2.5 mM, pH 7.0.

	λ_1 (nm)	***λ_2 (nm)***	***λ_3 (nm)***	***λ_4 (nm)***
$[Ag(BIA)_2]^+$	334	350	369	388
$[Ag(BIA)_2]^+$ / Tel-23	338 (+4)	356 (+6)	375 (+6)	395 (+7)
$[Ag(BIA)_2]^+$ / CTA-22	338 (+4)	354 (+4)	373 (+4)	394 (+6)
$[Ag(BIA)_2]^+$ / c-myc	337 (+3)	355 (+5)	374 (+6)	394 (+6)

Experimental details

Table S9 Melting temperatures of the different studied biosubstrates with their suitable buffer solutions.

Biosubstrate	**T_m (°C)**	**Buffer**
CT-DNA	59.8 ± 0.3	NaCac 2.5 mM, pH = 7.0
poly(rA)poly(rU)	56.3 ± 0.3	NaCl 0.1 M, NaCac 2.5 mM, pH = 7.0
poly(rA)2poly(rU)	56.0 ± 0.3	NaCl 0.1 M, NaCac 2.5 mM, pH = 7.0
Tel-23	62.8 ± 0.3	KCl 0.1 M, LiCac 2.5 mM, pH = 7.0
CTA-22	62.6 ± 0.2	KCl 0.1 M, LiCac 2.5 mM, pH = 7.0
c-myc	74.0 ± 0.4	KCl 0.01 M, LiCac 2.5 mM, pH = 7.0
i-motif	47.8 ± 0.1	NaCac 50 mM, pH = 5.5

Table S10 Sequences and Topologies of the double-labelled oligonucleotides used in this work.

Name	**Sequence (5' – 3')**	**Topology**
F21T	FAM-GGTTAGGGTTAGGGTTAGGG-TAMRA	Doubly labelled 3-tetrad Hybrid DNA G4 of human telomere
Fmit9438T	FAM-GGCGTAGGTTTGGTCTAGGG-TAMRA	Doubly labelled 2-tetrad Antiparallel mitochondrial DNA G4
F25CebT	FAM-AGGGTGGGTGTAAGTGTGGGTGGGT-TAMRA	Doubly labelled 3-tetrad Parallel DNA G4 of human minisatellite
F21CTAT	FAM-GGGCTAGGGCTAGGGCTAGGG-TAMRA	Doubly labelled 3-tetrad Antiparallel DNA G4 of human telomere
FTBAT	FAM-GGTTGGTGTGGTTGG-TAMRA	Doubly labelled 2-tetrad Antiparallel DNA G4 of Thrombin binding aptamer
FdxT	FAM-TATAGCTAT-hexaethyleneglycolTATAGCTATA-TAMRA	Doubly labelled Intramolecular duplex

K summary table

Table S11 Equilibrium constants 25 °C of $[Ag(BIA)_2]^+$/biomolecule systems. HypSpec® software values with a 1:1 stoichiometry. For DNA, RNA and BSA buffer solution Nacl 0.1 M, NaCac 2.5 mM, pH = 7.0; G4 buffer solution KCl 0.1 M, LiCac 2.5 mM, pH = 7.0; i-motif NaCac 50 mM, pH = 5.5.

	K(10^5 M^{-1})
DNA double helix	0.095 ± 0.005
RNA double helix	-
RNA triple helix	-
G4 Tel-23	18 ± 5
G4 CTA-22	8.7 ± 0.8
G4 c-myc	7.2 ± 0.8
i-motif	0.32 ± 0.07
BSA	19.2 ± 0.7